

# Inclusive and exclusive measurements of high energy $\gamma$ -rays in the 101 MeV $^{19}\text{F} + ^{181}\text{Ta}$ fusion reaction

N. Gelli<sup>1</sup>, F. Lucarelli<sup>1</sup>, M. Cinausero<sup>2</sup>, E. Fioretto<sup>2</sup>, G. Prete<sup>2</sup>, D. Fabris<sup>3</sup>, M. Lunardon<sup>3</sup>, G. Nebbia<sup>3</sup>, G. Viesti<sup>3</sup>, D. Bazzacco<sup>3</sup>, C.A. Ur<sup>3</sup>, D.R. Napoli<sup>2</sup>, P. Pavan<sup>3</sup>, C. Rossi Alvarez<sup>3</sup>, P.F. Bortignon<sup>4</sup>, E.M. Fiore<sup>5</sup>, L. Fiore<sup>5</sup>, V. Paticchio<sup>5</sup>, B. Fornal<sup>6</sup>

<sup>1</sup> I.N.F.N. and Dipartimento di Fisica dell'Università di Firenze, Firenze, Italy

<sup>2</sup> I.N.F.N., Laboratori Nazionali di Legnaro, Legnaro, Italy

<sup>3</sup> I.N.F.N. and Dipartimento di Fisica dell'Università di Padova, Padova, Italy

<sup>4</sup> I.N.F.N. and Dipartimento di Fisica dell'Università di Milano, Milano, Italy

<sup>5</sup> I.N.F.N. and Dipartimento di Fisica dell'Università di Bari, Bari, Italy

<sup>6</sup> Institute of Nuclear Physics, Krakow, Poland

Received: 14 September 1999 / Revised version: 17 December 1999

Communicated by D. Schwalm

**Abstract.** The high energy  $\gamma$ -rays from the fusion-evaporation reaction 101 MeV  $^{19}\text{F} + ^{181}\text{Ta}$  have been measured in coincidence with different  $\gamma$ -ray fold windows or discrete  $\gamma$ -rays in final residual nuclei. The line-shape analysis of the high energy  $\gamma$ -ray spectra confirms the large deformation of the  $^{200}\text{Pb}$  nuclei at high angular momenta. Coincidences with discrete  $\gamma$ -transitions evidence a strong correlation between  $\gamma$ -rays in the Giant Dipole Resonance region ( $E_\gamma \geq 8$  MeV) and final evaporation residues.

**PACS.** 24.30.Cz Giant resonances – 25.70.Gh Compound nucleus

## 1 Introduction

The study of the high energy  $\gamma$ -rays emitted in heavy-ion reactions provides valuable informations on the properties of highly excited nuclei. In particular, the energy range  $E_\gamma \geq 8$  MeV has a special interest, being related to the decay of the Giant Dipole Resonance (GDR) states. The parameters characterizing the GDR (energy  $E_D$ , width  $\Gamma$  and strength  $S$ ) depend on fundamental collective nuclear properties such as the symmetry energy, the size and the shape of the nuclei and the coupling of the collective motion to the surface vibrations. The systematic study of the GDR parameters performed in the past, mainly based on inclusive measurements, provided a detailed picture of the evolution of collective nuclear properties as a function of angular momentum and temperature [1].

Only a few exclusive GDR measurements have been performed so far, detecting high energy  $\gamma$ -rays in coincidence with evaporation residues (ER) [2–4] or fission fragments [5]. In recent years, a renewed interest on these exclusive studies was generated by the availability of high efficiency Germanium  $\gamma$ -ray spectrometers [6–13]. The gating on discrete  $\gamma$ -ray transitions is, indeed, an useful way to tag the reaction channel and to search for possible correlations between the decay of GDR states and the population of particular ER's. This technique is most effective when only few evaporation channels are open, as in the

decay of compound nuclei (CN) at medium-low excitation energy, being the  $\gamma$  spectra relatively simple in the latter case. The selection of angular momentum regions in the compound system is also possible when the spectrometers are equipped with ancillary  $4\pi$  multiplicity filters.

The comparison between these highly exclusive experimental data and theoretical predictions is an important tool for testing the reliability and the limitations of the actual Statistical Model (SM) calculations [9,11] that describe the CN decay. The latter data are, in fact, not affected by contaminations from reaction channels different from the CN decay that have been evidenced in some of the past inclusive experiments.

In this paper, we present a new set of selective experimental data aimed at verify and extend our actual knowledge on the energetic  $\gamma$ -ray production in heavy-ion reactions. For this purpose, a new investigation of the inclusive and exclusive channels in the high energy  $\gamma$ -ray emission from the  $^{19}\text{F} + ^{181}\text{Ta}$  reaction was carried out at the  $4\pi$   $\gamma$ -ray spectrometer GASP. The  $^{19}\text{F} + ^{181}\text{Ta}$  reaction was chosen because of the existing inclusive [14,15] and fission fragments coincidence studies [5] of the high energy  $\gamma$ -ray emission. All these works evidenced a transition of the  $^{200}\text{Pb}$  compound nuclei from spherical to highly deformed ( $\beta \sim 0.3$ ) shapes, induced by angular momentum effects.

## 2 Experimental details

The experiment was performed at the XTU Tandem facility of the Laboratori Nazionali di Legnaro. A 101 MeV  $^{19}\text{F}$  beam with an intensity of about 100 nA was focused onto a self supporting  $620 \mu\text{g}/\text{cm}^2$   $^{181}\text{Ta}$  target. The corresponding excitation energy of the populated  $^{200}\text{Pb}$  CN is  $E_x=65$  MeV. The chosen bombarding energy optimizes the evaporation-to-fission ratio, populating angular momenta in the fusion-evaporation channel up to the maximum allowed value  $J_{ER} \simeq 31\hbar$ . In fact, the measured cross section for fusion-evaporation reaches its maximum value ( $\sim 300$  mb) at the bombarding energy  $\sim 100$  MeV, whereas the fusion-fission contribution is only the 25% of the total fusion cross section [16].

Low energy ( $E_\gamma < 4$  MeV)  $\gamma$ -rays were detected with the GASP spectrometer [17] which consists of an array of 40 large volume Compton suppressed High Purity Germanium detectors (HPGe), positioned in 7 rings at different angles with respect to the beam direction, and of an inner ball of 80 Bismuth Germanate (BGO) scintillators.

Two large volume (10 cm  $\times$  10 cm) cylindrical BGO crystals, temperature stabilized and gain monitored, have been used to detect the high-energy  $\gamma$ -rays. Both scintillators were positioned at 75 cm from the target replacing two HPGe detectors of the array at  $\theta=90^\circ$  and  $145^\circ$ . The time-of-flight technique, with the start signal given by the inner ball, was used to distinguish  $\gamma$ -rays from neutrons.

High energy  $\gamma$ -ray events were recorded under the condition that at least 3 inner ball elements and 1 HPGe detector fired in coincidence with one large BGO. Events in which at least 2 HPGe detectors and 3 inner ball elements fired in coincidence were also collected.

The HPGe detectors were calibrated using a combination of standard radioactive sources and known in-beam  $\gamma$ -lines. The calibration of the large volume BGO detectors was performed using  $^{60}\text{Co}$  and  $^{56}\text{Co}$  sources, the 7.4 and 10.2 MeV  $\gamma$  peaks originating from slow neutron capture in the Ge isotopes of the crystals [18].

In the off-line analysis, the  $\gamma$ -ray spectra measured in the two detectors were added in order to increase the total statistics. For this purpose, a Doppler shift correction for the velocity of the compound nucleus was applied in the case of the backward BGO.

The HPGe data were used to build  $E_\gamma$ - $E_\gamma$  matrices and  $E_\gamma$ - $E_\gamma$ - $E_\gamma$  cubes with various conditions on the  $\gamma$ -ray fold  $k$  measured in the inner ball. Cubes and matrices were also generated by using coincidences between the high energy  $\gamma$ -rays measured in one of the large volume BGO detectors, the low energy  $\gamma$ -rays measured in the HPGe detectors and/or the fold  $k$  measured in the inner ball.

## 3 Results and Discussion

### 3.1 Line-shape analysis of the inclusive high energy $\gamma$ -ray spectra

As a first step of our analysis, we have studied the inclusive high energy  $\gamma$ -ray spectra, i.e. the spectra with only

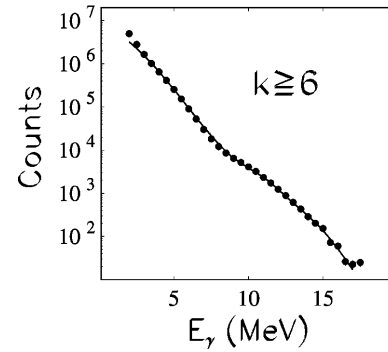


**Fig. 1.** Inclusive high energy  $\gamma$ -ray spectrum for fold  $k \geq 6$ . The solid line is the result of a two-lorentzian fit to the experimental spectrum. For detail see the text

the selection of the fold  $k$  measured in the GASP inner ball. For such a study, the lower folds ( $k \leq 5$ ) can not be considered. The inspection of the HPGe  $\gamma$ -ray spectrum reveals, indeed, large structures which are believed to be produced in two-body reaction channels. In fact, due to the wide spread of directions and velocities of the reaction products, the discrete  $\gamma$ -rays from these channels are not properly Doppler corrected when the CN velocity vector is assumed for the emitting source [6]. On the contrary, the discrete transitions in the evaporation residues dominate the  $\gamma$ -ray spectrum in coincidence with the higher folds ( $k \geq 6$ ).

The GDR parameters for a two-lorentzian strength distribution were obtained by fitting the experimental high fold inclusive spectrum ( $k \geq 6$ ) with the one resulting from CASCADE [19] SM calculations folded with the detector response function. A level density parameter value  $a=A/8$   $\text{MeV}^{-1}$  was used in the calculations to allow a direct comparison with the findings of [5, 14, 15]. The angular momentum region corresponding to the fold selection was taken into account by using the average fold-to-spin conversion reported in [20].

The result of the two-lorentzian fit to the  $k \geq 6$  high energy  $\gamma$ -ray spectrum is reported in Fig. 1. The obtained GDR parameter values are: strength  $S=1.0 \pm 0.1$  EWSR units, centroid energy of the first (second) component  $E_1=11.7 \pm 0.3$  MeV ( $E_2=15.0 \pm 0.5$  MeV), width of the first (second) component  $\Gamma_1=3.9 \pm 0.4$  MeV ( $\Gamma_2=4.8 \pm 0.5$  MeV). The quoted errors take also into account the uncertainties due to the used average fold-to-spin conversion. The reduced  $\chi^2$  value for this fit is  $\chi^2/\nu=1.3$ .

The fraction of the strength  $S$  in the second GDR component is found to be  $F_2=0.67 \pm 0.05$ , suggesting a prolate collective deformation of the CN. The splitting between the two centroid energies,  $E_1$  and  $E_2$  calculated with the Danos formula [21] provides an estimate of the quadrupole deformation parameter value  $\beta=0.29 \pm 0.08$ , in nice agreement with the results reported in [14].

In principle, the present experimental set-up allow the direct study of the angular momentum dependence of the GDR parameters [6]. In fact, high energy  $\gamma$ -ray spectra with different fold  $k$  selections sample the GDR in different angular momentum regions. However, the previously

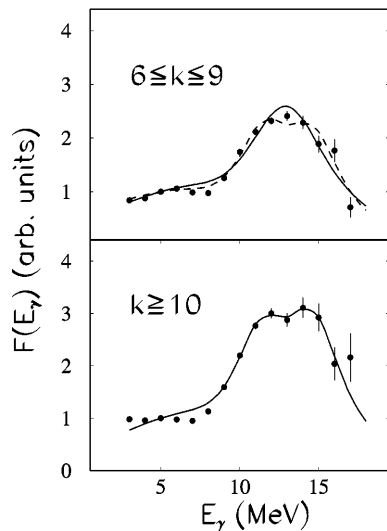


**Fig. 2.** Linearized plots of the high energy  $\gamma$ -ray spectra for fold  $6 \leq k \leq 9$  and  $k \geq 10$ . Lines are the results of statistical model fits (solid two-lorentzian, dashed one-lorentzian) to the experimental spectra. The linearization was obtained by dividing each spectrum (experimental and the best fit) by a calculated one in which the GDR strength is set to zero

discussed exclusion of the low folds ( $k \leq 5$ ) from our analysis, implies that we are scarcely sensitive to the low angular momentum region where the CN is believed to retain its ground state spherical shape [15]. An additional limitation to our sensitivity comes from the collected statistics which does not allow the use of narrow fold  $k$  bins to perform a GDR parameter search within a reasonable uncertainty level. A compromise between the collected statistics and the need of further unpacking the data is obtained by considering the two fold regions:  $6 \leq k \leq 9$  and  $k \geq 10$ . The first window samples the angular momentum region  $10\hbar \leq J \leq 17\hbar$ , the upper limit being in the range of the reported value for the spherical to deformed transition  $L_c \sim 13 \div 17\hbar$  [15]. The second condition selects the angular momentum region above  $17\hbar$  where the composite system is supposed to be strongly deformed.

The line-shape of the corresponding  $\gamma$ -ray spectra has been analyzed assuming both one- and two-lorentzian GDR strength distributions, which are characteristic of spherical and deformed shape, respectively. The best-fit spectra, reported in Fig. 2, evidence that, as expected, a two-lorentzian GDR distribution nicely reproduces the line-shape of the experimental spectrum for  $k \geq 10$ . In this case, the best fit values of the GDR parameters are very similar to the ones reported for the  $k \geq 6$  case discussed previously. On the contrary, for the lower fold window both, one- and two-lorentzian, fits give a poor reproduction ( $\chi^2/\nu \sim 10$ ) of the experimental  $\gamma$  spectrum.

The latter result does not allow to distinguish between the two possible shapes and can be taken as an indication that the contribution from nearly spherical shapes is not the dominant one in the  $6 \leq k \leq 9$  fold selection. Consequently, the balance between spherical and deformed shapes in the spin region selected by the  $6 \leq k \leq 9$  fold cut

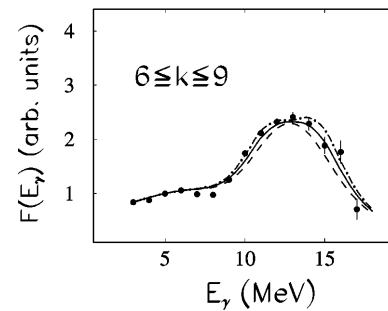


**Fig. 3.** Linearized plots of the high energy  $\gamma$ -ray spectra for fold  $6 \leq k \leq 9$ . Lines are the results of Statistical Model calculations in which the excited nucleus is assumed to be spherical for  $10\hbar \leq J \leq j_s$  and deformed for  $j_s \leq J \leq 17\hbar$ , where  $j_s = 12\hbar$  (dashed line),  $14\hbar$  (solid line) and  $16\hbar$  (dot-dashed line)

has been studied in more detail with CASCADE Statistical Model calculations assuming a one-lorentzian GDR strength distribution for the  $10\hbar \leq J \leq j_s$  spin range and a two-lorentzian distribution for the complementary region  $j_s \leq J \leq 17\hbar$ . The GDR parameters for one-lorentzian distribution are taken from [15], for two-lorentzian we used the parameters reported previously in this section. The predicted spectra were summed weighting over the spin dependent CN cross-section. The results of the calculations corresponding to  $j_s = 12\hbar$ ,  $14\hbar$  and  $16\hbar$  are compared with the experimental data in Fig. 3. From this comparison it is clearly seen that a good agreement between data and predictions is achieved for  $j_s = 14\hbar$  which is in the range of the angular momentum value for spherical to deformed shape transition reported in the past [15].

### 3.2 High energy $\gamma$ -ray emission and the selection of evaporation chains

The present experimental set-up also offers the possibility to study the correlations between the emission of an energetic  $\gamma$ -ray in the GDR region ( $E_\gamma \geq 8$  MeV) and the population of final evaporation residues. This task is performed by considering the coincidences between  $\gamma$ -rays detected in the large volume BGO scintillators and discrete transitions in the GASP HPGe detectors. The same method was applied in recent years [6, 9, 11, 13] showing that the line-shape of the high energy  $\gamma$ -ray spectra is strongly dependent from the selected evaporation residues. Similar results were obtained in an earlier measurement employing a different experimental technique for the evaporation residue selection [3]. Furthermore, it has to be noticed that Monte Carlo SM calculations were able to provide a realistic account of the exclusive high-energy  $\gamma$ -ray spectra in the mass region  $A \sim 150$  [9, 11].

In the case of the decay of the  $^{200}\text{Pb}$  at  $E_x = 65$  MeV, only few  $xn$  channels contribute to the total evaporation residue cross section, being negligible the charged particle evaporation. This is, indeed, an ideal situation to look for changes in the low energy  $\gamma$ -ray spectrum measured with the HPGe when a coincidence with  $\gamma$ -rays of different energies in the large BGO detectors is required. As

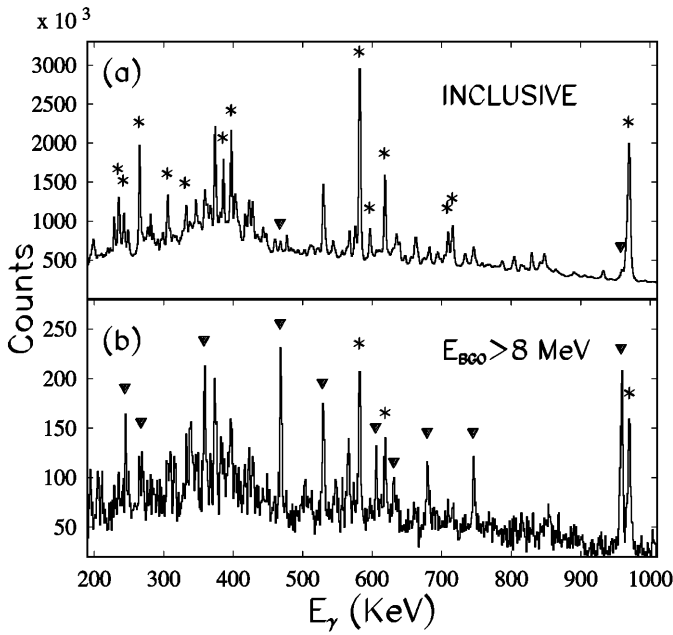


**Fig. 4.** Low energy  $\gamma$ -ray spectra from the HPGe detectors. Inclusive HPGe spectrum is shown in the (a) panel. In panel (b) a coincidence with a  $\gamma$ -ray of energy  $E_{\gamma} \geq 8$  MeV is required. Stars (full triangles) mark discrete transitions on  $^{195}\text{Pb}$  ( $^{196}\text{Pb}$ ) nuclei

shown in Fig. 4, the discrete  $\gamma$ -transitions in the main evaporation residue  $^{195}\text{Pb}$  ( $5n$  decay channel) dominate the HPGe spectrum when no energy selection is required in the BGO detectors. On the other hand, discrete lines in the  $^{196}\text{Pb}$  residual nucleus ( $4n$  decay channel) are strongly enhanced when a  $\gamma$ -ray of energy  $E_{\gamma} \geq 8$  MeV is detected in the large volume scintillators.

The change of the relative intensity between the  $5n$  and the  $4n$  channels as a function of the  $\gamma$ -ray energy measured in the large BGOs is illustrated in detail in Fig. 5 where the  $2^+ \rightarrow 0^+_{g.s.}$  969 keV transition in  $^{195}\text{Pb}$  is compared to the  $14^+ \rightarrow 12^+$  958 keV  $\gamma$ -line in  $^{196}\text{Pb}$ , which populates the isomeric state ( $T_{1/2} = 270$  ns) at  $E_x = 2693$  keV.

As estimated from the ratio between the integrals of the two lines, the  $4n/5n$  ratio increases by about one order of magnitude (from  $\sim 0.1$  to  $\sim 1$ ) considering the lowest ( $2 \text{ MeV} \leq E_{\gamma} \leq 4 \text{ MeV}$ ) and the higher  $8 \text{ MeV} \leq E_{\gamma} \leq 12 \text{ MeV}$  energy coincidence requirements. The  $^{195}\text{Pb}$  line disappears for the highest energies ( $E_{\gamma} \geq 12 \text{ MeV}$ ).

The results in Fig. 5 are complementary to the observation that the experimental sensitivity to the GDR strength function could be enhanced when looking to particular decay chains [3,9]. This effect is explained by noting that a  $\gamma$ -ray from the GDR decay carries energy and spin comparable to that of an evaporated neutron. Thus, the population of residual nuclei coming from the shorter  $xn$  chains is enhanced when, in the CN decay, an energetic  $\gamma$ -ray is emitted.

The high energy  $\gamma$ -ray spectra in coincidence with discrete  $\gamma$ -transitions in  $^{195}\text{Pb}$  and  $^{196}\text{Pb}$  residual nuclei are presented in Fig. 6 compared with the inclusive ( $k \geq 6$ )

spectrum. To derive such spectra, the  $E_{\gamma}$ - $E_{\gamma}$  matrix obtained from the HPGe data has been used to verify that the discrete transitions chosen for the selection of the  $^{195}\text{Pb}$  and  $^{196}\text{Pb}$  nuclei are not contaminated by transitions of similar energies in other reaction products.

As already discussed, the  $5n$  channel shows a reduced relative yield in the GDR region ( $E_{\gamma} \geq 8 \text{ MeV}$ ) with respect to the statistical region ( $4 \text{ MeV} \leq E_{\gamma} \leq 6 \text{ MeV}$ ) as compared to the inclusive  $k \geq 6$   $\gamma$ -ray spectrum. On the contrary, this relative yield is enhanced by about a factor 6 when the  $4n$  channel is considered. This experimental trend is qualitatively accounted for by SM Monte Carlo simulations [9] in which the GDR parameters extracted in our inclusive measurements were used.

## 4 Summary

A new investigation of the high energy  $\gamma$ -ray emission in the  $101 \text{ MeV } ^{19}\text{F} + ^{181}\text{Ta}$  reaction performed at the GASP spectrometer is described in this work. Inclusive  $\gamma$ -ray spectra were obtained by setting gates on the fold  $k$  measured in the GASP inner ball. Exclusive spectra were also obtained by requiring the coincidence with discrete transitions in  $^{195}\text{Pb}$  and  $^{196}\text{Pb}$  residual nuclei.

The GDR line-shape analysis of the inclusive spectra demonstrates that the source of the GDR photons is strongly deformed when high angular momentum states are selected. This is in nice agreement with findings of earlier studies of the same system [14,15]. In those experiments, the study of the spectra measured at different bombarding energies suggested a transition between nearly spherical and deformed shapes in the range  $13 \div 17\hbar$ . The collected statistics and the exclusion of the low folds ( $k \leq 5$ ), due to background problems, limited our experimental sensitivity in the low angular momentum region in which the nucleus retains the ground-state spherical shape. However, a detailed study performed with Statistical Model calculations is consistent with a shape transition at an angular momentum of about  $14\hbar$ . Recent measurements of high energy  $\gamma$ -rays for the  $^{16}\text{O} + ^{181}\text{Ta}$  system [22] suggest that this shape change with spin is a general feature in the  $A \sim 200$  mass region.

Exclusive channels were studied looking either to the HPGe spectra as a function of the energy of the  $\gamma$ -rays detected in the large BGO's or to the high-energy  $\gamma$ -ray spectra in coincidence with discrete transitions in the main evaporation residues. The results shown here demonstrate that the ratio between the  $\gamma$ -ray yield in the GDR region ( $E_{\gamma} \geq 8 \text{ MeV}$ ) and that in the statistical part of the spectrum ( $4 \text{ MeV} \leq E_{\gamma} \leq 6 \text{ MeV}$ ) is enhanced when triggering on the shorter  $xn$  evaporation chains. This is of special interest for GDR line-shape studies because it provides a strong reduction of the background due to the statistical  $\gamma$ -ray emission. Furthermore, the shorter evaporation channel is naturally located at the highest angular momenta populated in the fusion-evaporation, thus sampling the largest deformations.

The analysis of the exclusive data requires Monte Carlo versions of the SM codes in which the filtering of the events

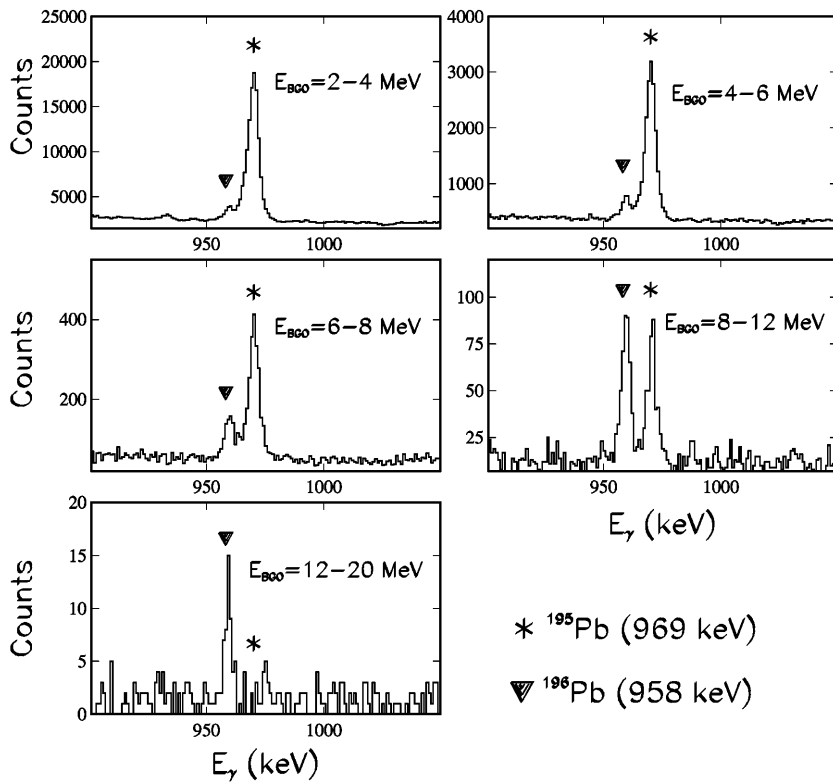


Fig. 5. Balance between the 969 keV transition in  $^{195}\text{Pb}$  and the 958 keV transition in  $^{196}\text{Pb}$  as a function of the  $\gamma$ -ray energy detected in the large BGOs

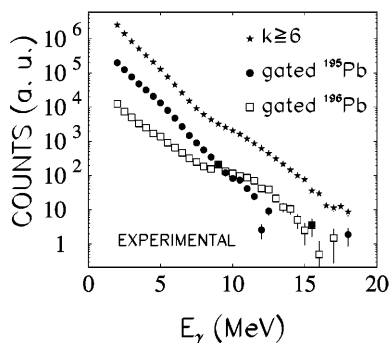


Fig. 6. Comparison between inclusive ( $k \geq 6$ ) and exclusive ( $4n$  and  $5n$  decay channels) experimental high energy  $\gamma$ -ray spectra

can be possible to reproduce the experimental conditions. The Monte Carlo simulation of high-energy  $\gamma$ -ray spectra is time consuming, because of the low probability of this emission and in very few cases the comparison with experimental data has been done. Nevertheless, in a next future, it seems to be of great interest to look at the nuclear deformations in specific exclusive channels by using improved Monte Carlo simulations of  $\gamma$ -ray emission.

We would like to thank the accelerator crew of the Tandem XTU in Legnaro for providing good beam quality and efficient operation during the experiment. Thanks are also due to A. Buscemi, M. Caldogno and R. Isocrate for the technical support in the preparation of the experiment.

## References

1. See e.g.: *Proceedings of the Conference on Giant Resonances, Groningen, The Netherlands, 28 June - 1 July, 1995* Nucl. Phys. A599 (1996)
2. A. Stolk, et al., Nucl. Phys. A505, 241 (1989)
3. A. Atac, et al., Phys. Lett. B252, 545 (1990)
4. J.P.S. van Schagen, M.N. Harakeh, W.H.A. Hesselink, R.F. Noorman, Nucl. Phys. A581, 145 (1995)
5. R. Butsch, M. Thoennessen, D.R. Chakrabarty, M.G. Herman, P. Paul, Phys. Rev. C41, 1530 (1990)
6. G. Viesti, et al., Nucl Phys. A604, 81 (1996)
7. S. Flibotte, et al., Phys. Rev. Lett. 77, 1448 (1996)
8. S. Flibotte, et al., Phys. Rev. C53, R533 (1996)
9. G. Viesti, B. Fornal, M. Cinausero, Phys. Rev. C55, 1594 (1997)
10. L.H. Zhu, et al., Phys. Rev. C55, 1169 (1997)
11. L.H. Zhu, et al., Nucl. Phys. A635, 325 (1998)
12. M. Cinausero, et al., Il Nuovo Cimento 111A, 613 (1998)
13. F. Camera, et al., Eur. Phys. J. A 2, 1 (1998)
14. D.R. Chakrabarty, M. Thoennessen, N. Alamanos, P. Paul, S. Sen, Phys. Rev. Lett. 58, 1092 (1987)
15. M. Thoennessen, et al., Phys. Rev. C37, 1763 (1988)
16. D.J.Hinde, J.R. Leigh, J.O. Newton, W. Galster, S. Sie, Nucl. Phys. A385, 109 (1982)
17. D. Bazzacco, et al., Phys. Lett. B309, 235 (1993)
18. W. Krolas, et al., Z. Phys. A344, 147 (1992)
19. F. Pühlhofer, Nucl. Phys. A280, 267 (1977)
20. G. Viesti, et al., in *Proceedings of the International Nuclear Physics Symposium, December 18-22, 1995, Bombay, India*, edited by M.A. Eswaran and R.K. Choudhury (Department of Atomic Energy, India), p. 342
21. M. Danos, Nucl. Phys. 5, 23 (1958)
22. D.R. Chakrabarty, et al., Phys. Rev. C53, 2739 (1996)